Malays. J. Bioeng. Technol. Vol. 2, No.1, (2025): 29-35
https://doi.org/10.70464/mjbet.v2i1.1545

MALAYSIAN JOURNAL OF BIOENGINEERING AND TECHNOLOGY

MJBeT Malaysian Journal of Bioengineering and Technology

Effect of Structural, Optical, and Antibacterial Properties of Various Zinc Oxide Morphologies

Arlina Ali[1,2,*], Hidayani Jaafar[1,2], Nadiah Ameram[2], Muhammad Azwadi Sulaiman[1,2], Nik Alnur Auli Nik Yusuf[2]

[1]*Intelligent Manufacturing Technology Research Group, Faculty of Bioengineering and Technology, University Malaysia Kelantan, 17600 Jeli Kelantan, Malaysia*
[2]*Faculty of Bioengineering and Technology, University Malaysia Kelantan, 17600 Jeli Kelantan, Malaysia*

**Corresponding author: arlina@umk.edu.my*

ARTICLE INFO

Received:5 November 2024
Accepted:24 November 2024
Online:29 March 2024
eISSN: 3036-017X

ABSTRACT

This study investigates the influence of different zinc oxide morphologies on their structural, optical, and antibacterial properties. These investigations have extensive antibacterial capabilities of zinc oxide (ZnO) nanostructures, effectively targeting various microorganisms prevalent in environmental settings, including soil, water, and food. The synthesis of ZnO nanostructures was conducted through a hydrothermal method, varying the pH from 8 to 12, using zinc chloride (ZnCl) and sodium hydroxide (NaOH) as precursors, and subjected to the 24-hour heating process at 180°C. The characterisation of the samples involved X-ray diffraction (XRD), Ultraviolet-Visible (UV-Vis) spectroscopy, and inhibition zones in Escherichia coli (*E. coli*) agar plates. The XRD pattern illustrated the hexagonal wurtzite structure of the ZnO nanostructure, with the average crystallite size calculated. UV-Vis spectroscopy indicated absorption peaks of ZnO around 300 to 400 nm, signifying a blue shift. Furthermore, optical band gaps, derived from UV spectroscopy, demonstrated an increment from 2.88 to 3.25 eV across all samples. The size of the inhibitions zone increased as the pH values of ZnO increased. ZnO shows increased inhibition zones with higher pH, hexagonal wurtzite structure, and increasing optical band gaps. The relationship between zinc oxide morphologies and their structural, optical, and antibacterial properties offers the development of ZnO-based materials with enhanced performance for biomedical, pharmaceutical, and environmental applications.

Keywords: Zinc Oxide; Hydrothermal; Antimicrobial; pH values; UV-Vis

1. Introduction

Inorganic metal oxide ZnO is increasingly used for antimicrobial applications. The main advantages of using inorganic oxides compared to organic antimicrobial agents are their stability, robustness, and long shelf life. ZnO is a direct band gap semiconductor with a band gap energy of 3.36 eV, a high exciton binding energy of 60 meV at room temperature, and a high dielectric constant [1]. ZnO is relatively environmentally friendly because it is non-toxic, biocompatible, and stable at biological pH values [2].

In the past few decades, as compared to other metal oxides exhibiting anti-bacterial properties, ZnO has proved more poisonous against bacteria and less responsive to human cells [3]. There are numerous studies regarding the antibacterial effect using ZnO; the focus has been *E. coli*, with relatively few reports on *Staphylococcus aureus* (*S. aureus*). The ability of ZnO depends on the particle size from 100 nm to 0.8 microns [4]. A reduction in particle sizes is associated with an increase in antimicrobial activity. Different nanostructures with varying sizes exhibit significantly different effects on antimicrobial activity, which affect the extent of contact with bacterial cells. Synthesis at different pH values alters the particle size of ZnO.

Furthermore, ZnO nanostructures have been prepared using the vapour-liquid-solid method, chemical vapour deposition, sol-gel, electrodeposition, sonochemical, and spray pyrolysis [5]. Among these methods, the hydrothermal method is promising for fabricating ideal nanomaterials with unique morphology because of the low cost, low temperature, high yield, scalable process [2] and high purity advanced materials with control in the nanostructure and surface properties [1]. Hydrothermal methods are more convenient and less expensive than physical methods in controlling grain size and morphology. The hydrothermal method is a powerful and versatile technique for materials synthesis. It offers precise control over the growth and formation of materials, allowing the production of tailored materials with improved properties [6]. With its wide range of applications and scalability, the hydrothermal method significantly advances various fields, including materials science, chemistry, nanotechnology, and energy research.

In this work, we investigate the antimicrobial, structural, and optical properties by controlling the nanostructures using the hydrothermal method and by adjusting the pH of the solution. The results show that the pH values increased the antimicrobial activity, and the structure and optical properties were enhanced for all samples.

2. Materials and Methods

The nanostructures of ZnO were prepared from 12-gram ZnCl and 5-gram ammonium hydroxide (NH_4OH) [7]. The mixed solution was stirred for 1 hour at room temperature to achieve homogenisation. The pH was adjusted at pH 8, pH 9, pH 10, pH 11 and pH 12 by controlling the amount of ammonium hydroxide solution. Then, the solutions were heated using a Teflon-lined steel autoclave at 180°C for 24 hours. The precipitate obtained was washed 3 times with ethanol and distilled water. After being washed 3 times, precipitation was filtered with a vacuum pump, followed by drying at 60°C for 12 hours and examined in terms of their structural and physical properties.

The antibacterial activity of ZnO was evaluated against *E. coli* using a culture-based assay. *E. coli* samples were added to the nutrient broth and incubated in an orbital shaker at 37°C for 24 hours to promote bacterial growth. The bacterial culture was then streaked onto the surface of an agar plate using a sterile loop in a zigzag pattern to ensure uniform distribution. The plates were incubated at 37°C for 24 hours to allow bacterial growth on the culture media. To assess antibacterial activity, sterile paper discs were immersed in ZnO solution, distilled water (negative control), and chloramphenicol (positive control). The discs were placed onto the agar surface using sterile forceps, ensuring proper contact with the media. After incubation, the formation of a clear zone (zone of inhibition) around each disc indicated antibacterial activity. The annular radius of the inhibition zone was measured to determine the zone diameter. This assay was performed to evaluate the effectiveness of ZnO under various parameters, with the inhibition zone serving as a key indicator of antibacterial activity. Notably, this method was distinct from the standard disk-diffusion method, as it focused on direct ZnO treatment and its antibacterial efficacy.

X-ray diffraction (XRD) pattern was recorded using Bruker D2 Phaser with Cu Kα radiation at the Brag angle ranging from 20° to 90°. XRD determined the crystallinity and phase formation phase. Absorbance spectra have been recorded using a UV-1280 Multipurpose UV-visible spectrophotometer. The samples' optical properties were also studied by the UV-visible (UV-vis) absorption in the range from 200 to 800 nm at room temperature [8].

eISSN Number: 3036-017X

3. Results and Discussion

Morphological images of preparation at pH values of 8, 9, 10, 11, and 12 can be seen in Fig. 1. The ZnO prepared at pH 8 was observed as a l rod-like structure, and pH 9 shows a spherical granular shape. The morphological images form a flower-like structure by increasing pH to 10, 11, and 12 for ZnO.

From the zone inhibition in the agar plate, we can see that the morphology of ZnO has different microbial activity. The antimicrobial activity of ZnO at different pH values against *E. coli*, the inhibition zone in the agar plate seen in Fig. 2. A clear disk was observed with ZnO at pH 11 and pH 12, showing a clearing disk, while another disk had different sizes of clear disk diameters. This bacterium causes food poisoning, a type of gastroenteritis with sudden symptoms. The antibacterial activity exhibited by ZnO could also be due to the presence of soluble Zn2+ or pH values since bacterial activity is sensitive to these factors. Enhancing microbial activity is mentioned in previous studies [9].

The (h,k,l) peaks of ZnO were detected at 2θ values of 31.7°, 34.4°, 36.2°, 47.5°, 56.6°, 62.8°, 66.3°, 67.9°, 69.0°, 72.5°, 76.9°, 89.6°, corresponding to the lattice planes (100), (002), (101), (102), (210), (103), (200), (212), (201), (004), (202), and (203) respectively. From the results, the increase in the intensity of the graph can be seen in Fig. 3 with increasing pH values. The sharp peak of the (101) plane in the XRD graph indicates a high crystalline structure of the samples. The intensity of the (101) plane is found to be maximum for all samples, and the intensity of the peak increases as the pH values increase, pH 9 < pH 10 < pH 11 < pH 12. The prominent peak of (101) and the absence of other peaks in the XRD graph indicate the purity of the sample [10].

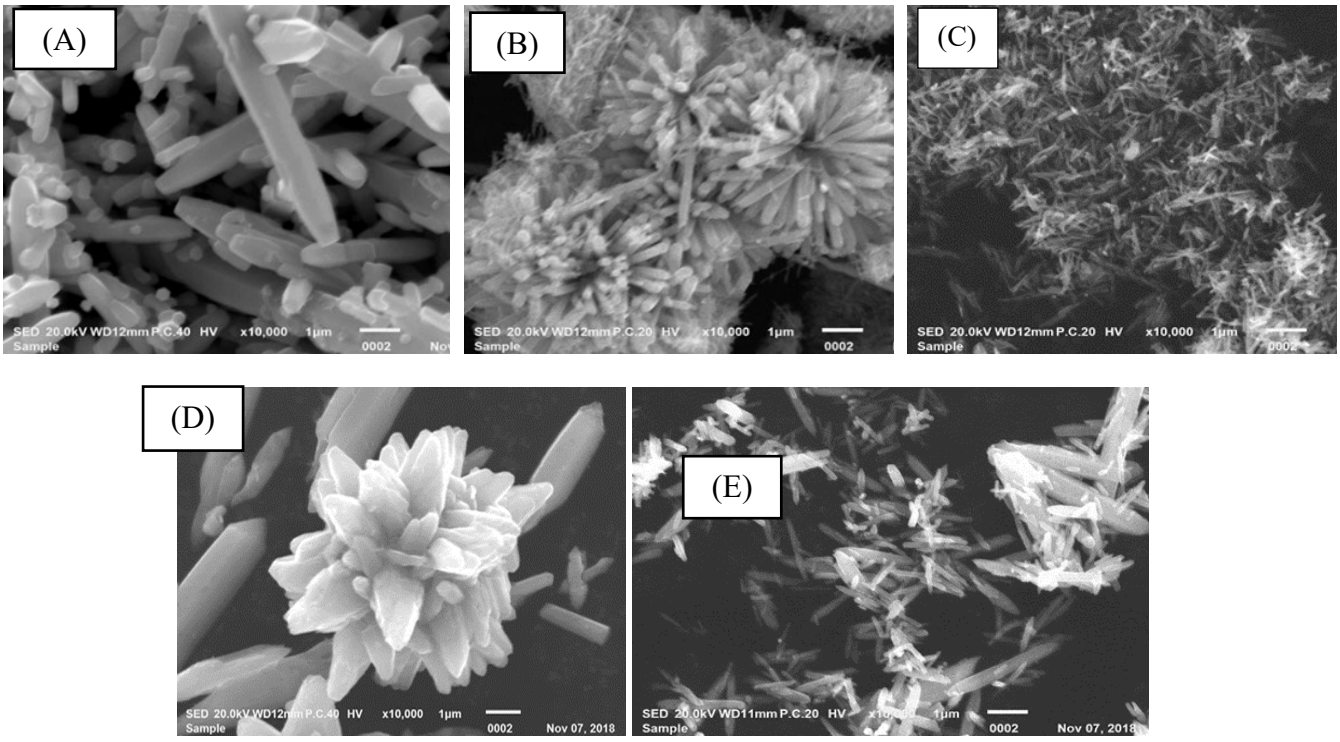

Fig. 1: Morphologies image of ZnO nanostructures prepared at different pH values: (A) pH 8, (B) pH 9, (C) pH 10, (D) pH 11, and (E) pH 12

eISSN Number: 3036-017X

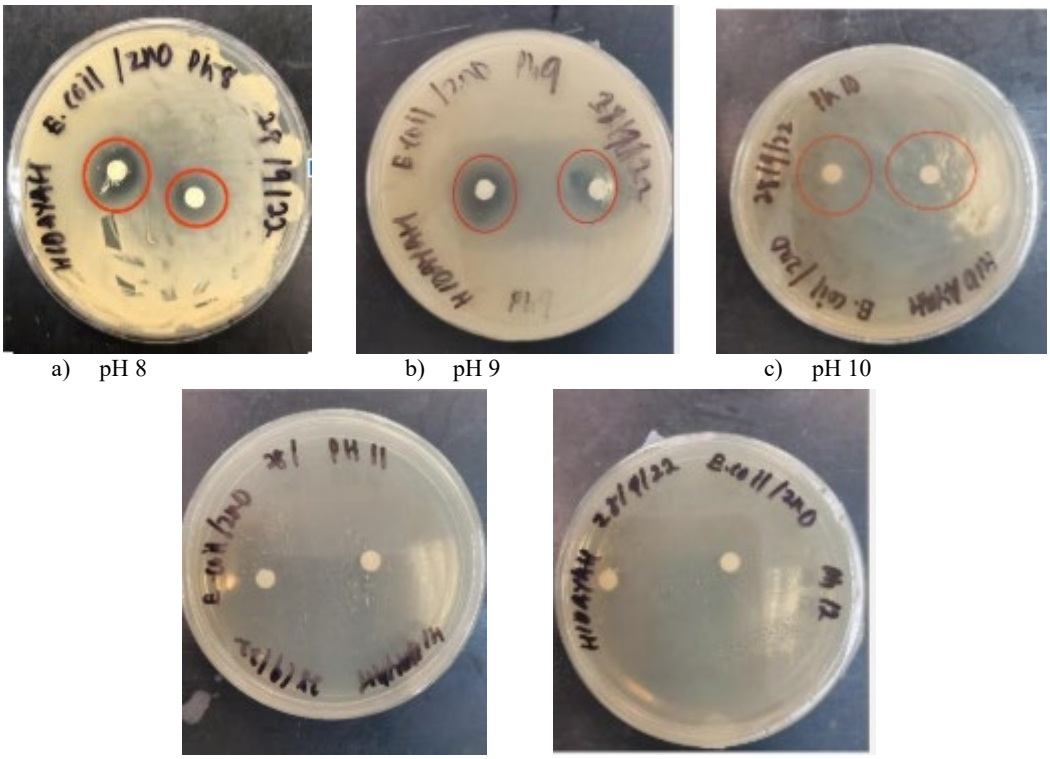

a) pH 8 b) pH 9 c) pH 10

d) pH 11 e) pH 12

Fig. 2: Zone of Inhibition for *E. coli* for ZnO nanostructures prepared at different pH values: (a) pH 8, (b) pH 9, (c) pH 10, (d) pH 11, and (e) pH 12

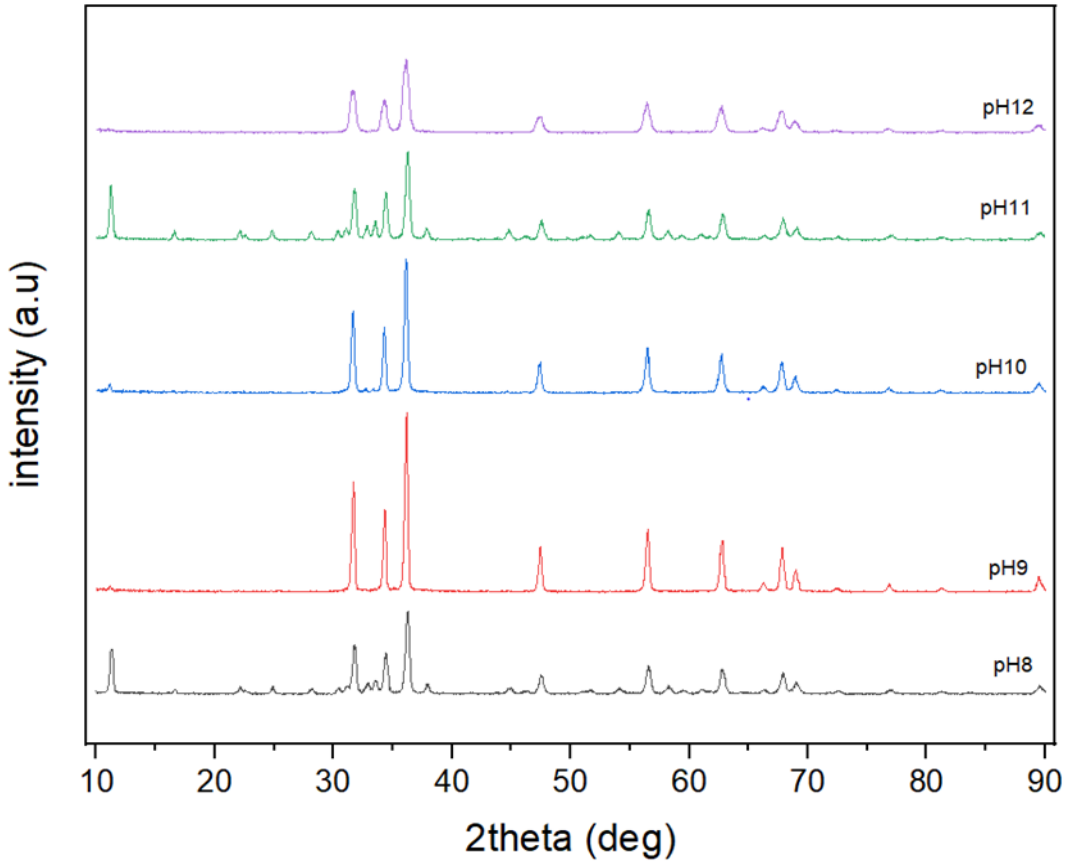

Fig. 3: X-ray diffraction pattern of ZnO nanostructures prepared at different pH values

eISSN Number: 3036-017X

The (101) plane, which is the highest peak, can be used to calculate the mean crystallite size of the prepared samples at various pH values using the Scherrer equation. The crystallite size for each sample is displayed in Fig. 4. The average crystallite size of ZnO with different pH was calculated using the Scherer formula as shown in Eq. (1).

$$D = k\lambda / (\beta \cos \theta) \quad \text{Eq. (1)}$$

Where D is crystallite size, λ for Cukα is 0.15406 nm, k is the crystallite shape factor, a good approximation is 0.9, whereas d is the value of full-width half maximum (FWHM), and θ is the angle in radians [11]. Fig.4 shows the formation of crystallite size increases when the pH values are increased. The crystallite sizes for pH 8, 9, 10, 11 and 12 of ZnO are 14.22, 19.96, 20.47, 21.86 and 25.21 nm, respectively. From there, the average crystallite size for ZnO nanostructures is 20.34 nm. The hexagonal wurtzite structure of ZnO has a lattice parameter constant of a=b= 3.249 Å and c=5.206 Å for all samples, as displayed in Table 1.

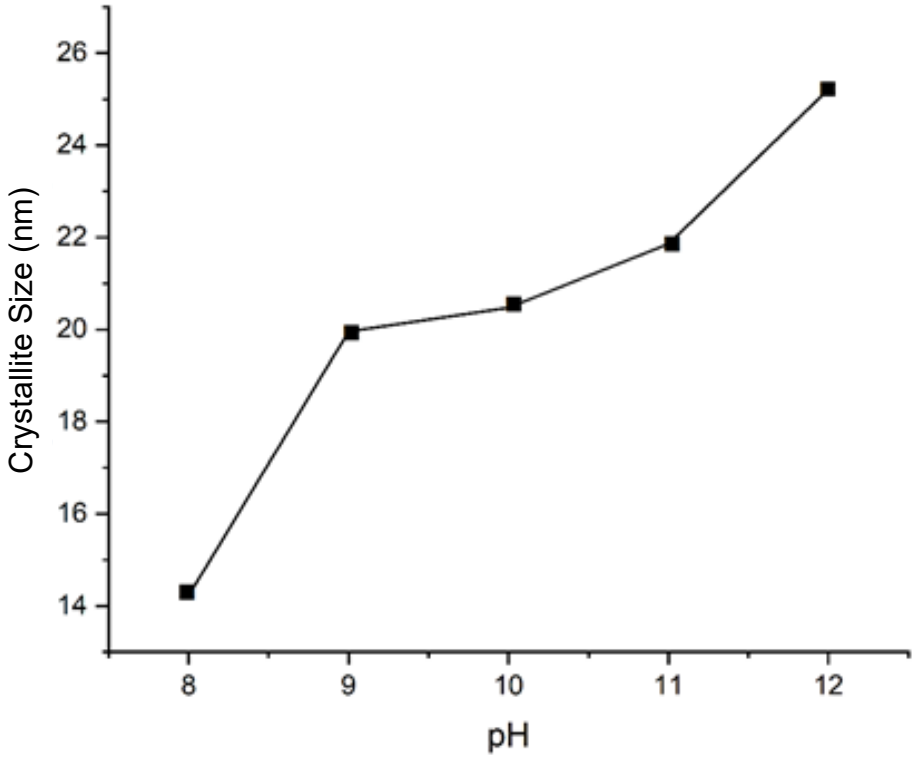

Fig. 4: Effect of pH values on crystallite size formations of ZnO nanostructures

Table 1 shows the results of the zone of inhibition by measuring the radius of the zone by creating contours and choosing the appropriate threshold value in mm. Growth inhibition zone of different pH values for ZnO as antibiotic strain against *E. coli* in disk diffusion. The growth bacteria for *E. coli* measuring the diameter of this zone on pH 8 were 2.0 mm, 2.5 mm for pH 9, and 4.0 mm for pH 10, and the zones are clearly visible for pH 11 and 12, shown in Fig. 2. Because the bacterium is sensitive to the ZnO, no growth will be observed. After a certain point, its concentration is so low that it can no longer inhibit the growth of the bacterium. Therefore, there is an area around the disks that will be clear against a dense growth of the bacterium surrounding it, this zone of clearance is defined as the zone of inhibition.

eISSN Number: 3036-017X

Table 1: Inhibition zone annular radius different pH value of ZnO nanostructure

pH	*Escherichia coli* Annular Radius (mm)
8	2.0
9	2.5
10	4.0
11	Clear
12	Clear

The effect of different pH values on the absorbance peaks of ZnO has been investigated based on the optical transmission spectrum by UV-visible spectroscopy at room temperature. The optical transmission spectrum of ZnO samples at different pH in the range of (200-800) nm is shown in Fig. 5. The average absorbance peak of ZnO is around 300 to 400 nm. The broad peak (or widening peak) indicates that ZnO nanoparticles absorb ultraviolet (UV) and visible light regions. The UV region covers the range of wavelength from 100-400 nm and is divided into three bands, which are Ultraviolet A (UVA), which has 315 - 400 nm; Ultraviolet B (UVB), which has 280-315 nm, and Ultraviolet C (UVC) 100 - 280 nm (WHO) [12,13]. At the same time, the visible region covers 380 to 700 nm wavelengths. As mentioned, ZnO nanoparticles that reflected at 300 to 400 nm lie between UVA and the blue region in the visible spectrum. This information describes the presence of a blue shift, which is important in determining the direct band gap of ZnO.

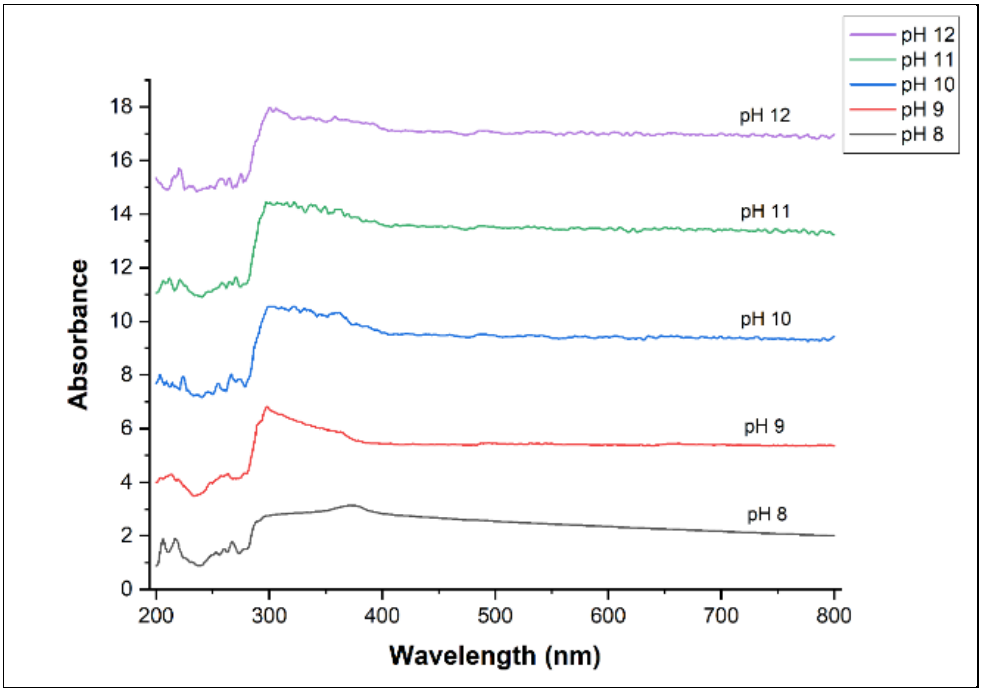

Fig. 5: The UV-Vis graph spectra of ZnO nanoparticles prepared different pH value of ZnO nanostructure

4. Conclusion

In conclusion, ZnO was successfully synthesised at different pH values using the hydrothermal method. The results demonstrated that increasing the pH values enhanced the structural and optical properties of ZnO. Additionally, morphological changes by pH value significantly influenced its antimicrobial activity against *Escherichia coli*. Therefore, pH values play a crucial role in determining the structural, morphology, optical, and antimicrobial properties of ZnO.

eISSN Number: 3036-017X

Acknowledgement

The authors thank Universiti Malaysia Kelantan (UMK) and Jordan University Science and Technology (JUST) for providing funding. This study was supported by the Matching Research Grant Scheme UMK-Jordan Grant number R/JUST/A1300/00356a/002/2023/01270. In addition, the authors want to thank Lim Ze Wen (J18B0248) for helping me accomplish this project.

References

[1] Chand P, Gaur A, Kumar A. Structural and optical properties of ZnO nanoparticles synthesized at different pH values. J Alloys Compd, 2012;539:174-178.

[2] Hu H, Huang X, Deng C, Chen X, Qian Y. Hydrothermal synthesis of ZnO nanowires and nanobelts on a large scale. Mater Chem Phys, 2007;106(1):58-62.

[3] Ijaz M, Zafar M, Islam A, Afsheen S, Iqbal T. A review on antibacterial properties of biologically synthesized zinc oxide nanostructures. J Inorg Organomet Polym Mater, 2020;30:2815-2826.

[4] Yamamoto O. Influence of particle size on the antibacterial activity of zinc oxide. Int J Inorg Mater, 2001;3(7):643-646.

[5] Abdulrahman AF, Ahmed SM, Hamad SM, Almessiere MA, Ahmed NM, Sajadi SM. Effect of different pH values on growth solutions for the ZnO nanostructures. Chin J Phys, 2021;71:175-189.

[6] Jensen KM, Tyrsted C, Bremholm M, Iversen BB. In situ studies of solvothermal synthesis of energy materials. ChemSusChem, 2014;7(6):1594-1611.

[7] Ali A, Yusoff M, Noor AAM, Ter Teo P, Mamat S, Mohamed M, Ramli NH, Akmal S. Synthesis of Zinc Oxide Nanostructures Growth by the role of pH variation. IOP Conf Ser Earth Environ Sci, 2020;596(1):012040.

[8] Saad IB, Hannachi N, Roisnel T, Hlel F. Optical, UV-Vis spectroscopy studies, electrical and dielectric properties of transition metal-based of the novel organic–inorganic hybrid $(C_6H_{10}N_2)(Hg_2C_{l5})_2.3H_2O$. J Adv Dielectr, 2019;9(05):1950040.

[9] Gharpure S, Ankamwar B. Synthesis and antimicrobial properties of zinc oxide nanoparticles. J Nanosci Nanotechnol, 2020;20(10):5977-5996.

[10] Kothawale RR, Mohite RM. Morphological, Electrical and Optical Properties of Al-Doped Zinc Oxide Nanorods. Adv Mater Res, 2015;1110:218-221.

[11] Singh A, Vishwakarma HL. Study of structural, morphological, optical and electroluminescent properties of undoped ZnO nanorods grown by a simple chemical precipitation. Mater Sci-Poland, 2015;33(4):751-759.

[12] Semenova NA, Smirnov AA, Ivanitskikh AS, Izmailov AY, Dorokhov AS, Proshkin YA, Yanykin DV, Sarimov RR, Gudkov SV, Chilingaryan NO. Impact of ultraviolet radiation on the pigment content and essential oil accumulation in sweet basil (*Ocimum basilicum L.*). Appl Sci, 2022;12(14):7190.

[13] Munawar T, Yasmeen S, Mukhtar F, Nadeem MS, Mahmood K, Saif MS, Hasan M, Ali A, Hussain F, Iqbal F. $Zn_{0.9}Ce_{0.05}M_{0.05}O$ (M= Er, Y, V) nanocrystals: structural and energy bandgap engineering of ZnO for enhancing photocatalytic and antibacterial activity. Ceram Int, 2020;46(10):14369-14383.

eISSN Number: 3036-017X